Analysis of Clipping Effect in Color Images Captured by CCD Cameras

Jae Byung Park
Robot Vision Laboratory
Purdue University, West Lafayette, IN. U.S.A.
jbpark@purdue.edu

Guilherme N. DeSouza
Vision-Guided & Intelligent Robotics Laboratory
University of Western Australia, Australia
gdesouza@ee.uwa.edu.au

Abstract

Camera sensors (CCD) have a limited dynamic range that constrains the brightness of the incident light that can be quantified. In other words, if the ray of incident light is too intense, the sensor saturates and the value quantified is inadequately represented. This color clipping effect is a common problem in computer vision and it can become specially difficult when dealing with specular objects against a low-intensity background. In this paper, we present a method for analyzing such clipping effects of CCD cameras appearing in color images. Using an averaging technique to estimate the color of the illuminant, we define two types of axes in the RGB color cube: the Illumination Axis and the Clipping Axis. Our study concludes the followings: 1) the clipped pixels from a dielectric object form one or two lines, depending on the number of color channels on which the clipping effect takes place; and 2) these lines are parallel to the Clipping Axes. These two properties allow for a framework for a color-based segmentation that works even in the presence of saturated (specular) regions in the image. Moreover, the captured images can now be obtained under a wider variation of illumination conditions.

INTRODUCTION

Any time we deal with bright incident light, the intensity of some pixels may exceed the dynamic range of the camera's CCD, which may no longer be able to capture a meaningful value for the incident light. In the case of color CCDs, this optical phenomenon is commonly known as color clipping effect. It may occur progressively in one, two or all three color channels (R, G, and B), depending, among other things, on the color of the illuminant [2]. In this paper, we analyze such clipping effect and we extract two properties of the pixels that can be used, for example, for segmentation of color objects under various illumination conditions.

Our analysis of the color clipping effect in images from a CCD sensing device can be best understood with the help of the dichromatic reflection model – first proposed by Shafer in [1]. For dielectric non-homogeneous materials, this model describes the reflected light as an additive mixture of two components: 1) the body reflectance component, and 2) the surface reflectance component:

$$L(\lambda, i, e, g) = m_b(i, e, g)c_b(\lambda) + m_s(i, e, g)c_s(\lambda) \qquad (1)$$

where $c_b(\lambda)$ and $c_s(\lambda)$ represent two distinct spectral power distributions. $L(\lambda, i, e, g)$ represents the intensity of reflected light at wavelength λ, where as i is the angle of incidence, e is the angle of reflection and g is the phase angle. Here m_b and m_s are geometric scale factors of the body reflectance component and the surface reflectance component respectively. If we include the spectral integration that takes place in the photo-optic sensors of a camera, we obtain the following simpler form for the recorded light:

$$C(x, y) = m_b(i, e, g)C_b + m_s(i, e, g)C_s \qquad (2)$$

where $C_b = [R_b, G_b, B_b]$ and $C_s = [R_s, G_s, B_s]$ are the body reflection vector and the surface reflection vector, respectively. What this equation tells us is that the color value $C(x, y)$ at pixel (x, y) is a weighted linear combination of the two vectors, C_b and C_s. In this model, the plane spanned by the two vectors, C_b and C_s is known as the dichromatic plane.

While it is true that the dichromatic reflection model represents a very useful approximation to the actual physics of light reflection, clipped color pixels do not follow the characteristics of this dichromatic reflection model. Moreover, simple processes such as color balancing and camera aperture control do not improve the dynamic range in the color channels and therefore they can not prevent clipping effects. In order to overcome these shortcomings, we must analyze the behavior of clipped pixels and determine any pattern in their position with respect to the dichromatic plane. Such analysis starts by estimating the color of the illuminant as it will be explained in the following section. Also, as depicted in Figure 1, our estimation process leads to the determination of two different axes in the RGB color cube: the illumination axis; and the clipping axis. As we will show later, we found that the direction of the cluster consisting of the clipped color pixels is not arbitrary, but instead it is well-defined, forming the orientation of the clipping axes. Finally, using multiple CCD cameras, we demonstrate how to exploit the correlation between the clipped color clusters and the clipping axes defined in the RGB color space for color-based segmentation.

ESTIMATION OF THE ILLUMINANT COLOR

Reflectance spectrophotometers and colorimeters have been commonly used for measuring the color of the illuminant [3]. A reflectance spectrophotometer scans different wavelengths of light reflected from the target surface and it records the intensity of that reflected light relatively to a standard white pattern. On the other hand, a colorimeter measures the tristimulus values more directly by using three broad-band filters. A colorimeter does not provide spectral reflectance

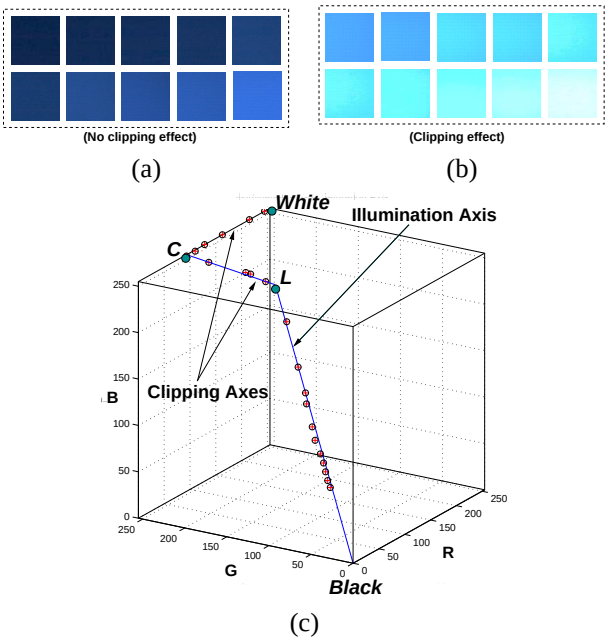

Figure 1. Determination of Illumination axis and clipping axes

(a) First train set of 10 images of the reflected light from a barium sulfate plate (a white reference plate) without any clipping effect; (b) Second train set of images with clipping effect; and (c) the illumination axis and the clipping axes estimated from the train sets given (a) and (b). The circled cross marks are the average color values of these 20 images shown in (a) and (b).

data, but the measured tristimulus values. Under ideally pure white illumination conditions, the color of the illuminant trivially varies along the gray axis in the RGB cube. However, if the color of the illuminant is non-white, that assumption is longer valid. This paper is primarily focused on such non-white, narrow-band illuminations. For these cases, we will show that it suffices to use standard CCD cameras in order to estimate the color of the illuminant.

We first discuss how to estimate the color of illuminant directly from a CCD camera by repeatedly measuring the color values of the reflected light from a planar surface covered with barium sulfate which is commonly used as a material that has purely white color. For each different illuminant, a training set of 20 images is recorded in the following manner: Conforming to the 10^o CIE standard observer, a digital camera is installed approximately $50cm$ away from the white reference plate. Images are captured from one of two viewing directions (approximately 0^o and 45^o to the surface normal of the reference plane). Figure 1 (a) and (b) show 20 such images of size 100x100 pixels retained from 20 different locations under blue colored incandescent lighting. For each such sampled image, the mean (μ_R, μ_G, μ_B) and the standard deviation $(\sigma_R, \sigma_G, \sigma_B)$ in the R, G, and B color channels are calculated. If at least one of the mean values is close to the max for a color channel, that indicates there is a deep-saturation caused by clipping effect in that channel. Such a patch for which this is true will participate in determination of the clipping axes. On the other hand, a patch needs to be discarded if the calculated mean for the patch is too close to zero for any of the three color channels[1]. Notice that the images in Figure 1 (a) exhibit no clipping effect whereas the images in Figure 1 (b) contain substantially large number of clipped pixels. Figure 1 (c) plots the average color values calculated from these patches. Then a linear least squares fitting technique was applied to the best fitting straight lines that define illumination axis and clipping axes for unsaturated and saturated pixels respectively.

The main idea is that for ordinary CCD cameras, the illuminant color variation in the RGB color cube can be modeled by a series of straight lines. In the next section, we discuss this idea in more detail.

THE ILLUMINATION AXIS AND THE CLIPPING AXES

In this section, we will show how the illumination axis and the clipping axes can be found in the RGB space. Based on our studies, all possible cases of the illumination and the clipping axes are listed below:

- Clipping effect in all three color channels simultaneously: In this case, the illumination axis coincides with the gray axis of the rgb cube. Moreover, the color of the illuminant is purely white and the clipping effect only occurs near to the "white point", and therefore the clipping axis becomes a single point (see Figure 2 (a));
- Clipping effect in two color channels simultaneously: The illumination axis intersects one of the three edges passing through the "white point" of the RGB cube. There is only one clipping axis defined along this edge of the cube (see Figure 2 (b));
- Clipping effect first in one single color channel: In this case, the clipping effect first occurs in one single color channel and then to the other two color channels. If the clipping occurs in all channels progressively, the illumination axis will cut one of the faces of the RGB cube and there will be two clipping axes as shown in Figure 2 (c): each one representing the subsequent clippings on the other two color channels. On the other hand, if the clipping occurs in a single channel first and later on the other two channels simultaneously, there will be only one clipping axis defined along the projection of the gray axis onto the face of the cube that was first intersected (see Figure 2 (d)).

For simplicity, we will limit our discussion to the case shown in Figure 2 (c) where the clipping effect occurs progressively in all three color channels. Also, for generality, we will use C_1, C_2, and C_3 to arbitrarily denote any of the three color channels – R, G, and B. In summary, we will assume that

[1]The following thresholds have worked well for us for detecting saturation and lack of adequate illumination: 1) over-saturation threshold: $max\,(\mu_R, \mu_G, \mu_B) \leq 252$; and 2) inadequate illumination threshold: $min\,(\mu_R, \mu_G, \mu_B) \leq 2$.

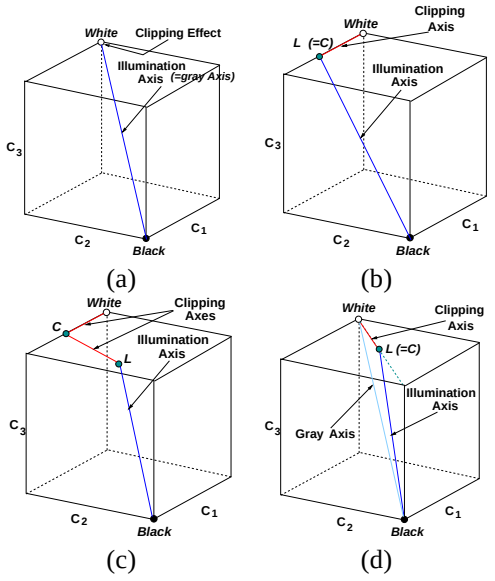

Figure 2. All possible cases of illumination axis and clipping axes (C_1, C_2, C_3 = three color channels)

the clipping effect first occurs in channel C_3, followed by channel C_2, and finally by channel C_1.

The results of estimating the color of the illuminants for six different scenes, each of which with a different illuminant, are tabulated in Table 1. The main purpose of the table is to show the directions of both illumination axis and clipping axes for various light sources and illumination conditions. The fourth column of this table shows the direction of the illumination axis, which starts at the origin of the RGB color cube and intersects one of the top faces of the RGB color cube (denoted as L in Figure 1 (c)). The line on the top face of the RGB cube that starts at point L and ends at point C in Figure 1 (c) defines the first clipping axis and is presented in the fifth column of Table 1. The second segment of the clipping axis, which may or may not exist, is the line from point C to the end of the RGB cube – denoted as $White$ in Figure 1 (c). We should also emphasize that in all experiments used for the construction of this table, white balancing and automatic gain control features of the cameras were disabled.

The reader should note that, in accordance to the dichromatic reflection model, the color cluster of unclipped specular pixels form a line parallel to the surface reflection vector C_s (see Eq. 2). This vector can be approximated by the illumination axis [4, 5, 6]. Also, since the CCD chip cells have limited dynamic ranges, both lines – the color cluster of non-saturated specular pixels and the illumination axis – present clipping effects. In the remaining of this section, we formally define the distance between these two parallel lines as clipping effect occurs. This distance can then be used, for example, as a threshold to segment the pixels from different object regions.

As we normalize the illumination axis L, we can define the unit vector $\overrightarrow{I}$ which has the same direction with the illumination L. Then the correlation between the unclipped specular pixels and the illumination axis L (using the unit vector $\overrightarrow{I}$) can be expressed as

$$C_{unclipped}(x,y) = m \cdot \overrightarrow{I} + \dot{n}_0 \tag{3}$$

$$= m \cdot \begin{bmatrix} l_R & I_G & I_B \end{bmatrix}^T + \begin{bmatrix} \dot{r} & \dot{g} & \dot{b} \end{bmatrix}^T \tag{4}$$

where m is a geometric scale factor and $\dot{n} = \begin{bmatrix} \dot{r} & \dot{g} & \dot{b} \end{bmatrix}^T$ is the discriminant point in the dichromatic plane where the color cluster of the unclipped specular pixels meets the mate pixels. Klinker and Shafer [2] have demonstrated that this discriminant point $\dot{n}$ can be found by convex hull fitting of these two components of the dichromatic reflection model. Then Eq. 4 can be re-written as

$$C_{unclipped}(x,y) = \begin{bmatrix} C_1 & C_2 & C_3 \end{bmatrix}^T \tag{5}$$

$$= m \cdot \begin{bmatrix} l_{C_1} & I_{C_2} & I_{C_3} \end{bmatrix}^T + \begin{bmatrix} \dot{c}_1 & \dot{c}_2 & \dot{c}_3 \end{bmatrix}^T \tag{6}$$

When C_3 gets clipped as the max of color channel, 255 is reached, we have $m \cdot I_{C_3} + \dot{c}_3 = 255$. Then the intersection point of the unclipped pixels $U = \begin{bmatrix} u_1 & u_2 & u_3 \end{bmatrix}^T$ (shown in Figure 3 (c)) can be calculated from Eq. 5:

$$U = \begin{bmatrix} u_1 & u_2 & u_3 \end{bmatrix}^T = 255 \cdot \begin{bmatrix} \frac{m \cdot l_{C_1} + \dot{c}_1}{m \cdot l_{C_3} + \dot{c}_3} & \frac{m \cdot l_{C_2} + \dot{c}_2}{m \cdot l_{C_3} + \dot{c}_3} & 1 \end{bmatrix}^T \tag{7}$$

The shortest distance calculated from U to the clipping axis that connects L and C is the displacement (denote as D in Figure 3) between the clipping axis and the line consists of the clipped pixels. The thresholds around this displacement value D will be used for our experiment in the next section is to segment the clipped pixels.

EXPERIMENTAL RESULTS

Figure 3 (a) shows the input image of two peppers (red and yellow) taken under blue colored illuminant. Figure 3 (c) presents the dispersion in the RGB space of the color clusters. These clusters form lines that are separate, but still parallel to the clipping axes.

[2].

Our analysis allows for the classification and segmentation of objects under various illumination conditions.For example, the classification of both unsaturated and saturated clipped pixels is shown in Figure 3 (c). The pixels are marked by white and black color respectively. Here, we must emphasize that we use two sets of clipping axes: one for clipped pixels from the red pepper and the other for the pixels from the yellow pepper. By doing so, our segmentation scheme is not only able to separate the clipped pixels from the unclipped pixels but also to determine to which region of the image each clipped pixel belongs. That is, from which of the two different colored peppers.

[2]Additional results using various objects, multiple cameras, and different illuminants are available at: (http://rvl1.ecn.purdue.edu/RVL/newcolorspace).

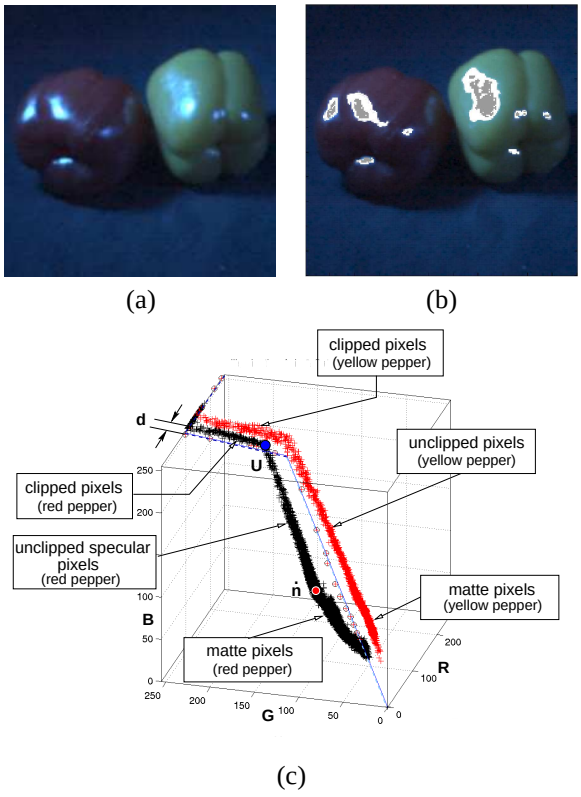

Figure 3. Experimental result

(a) The input images with two peppers (yellow and red); (b) The detected specular pixels where the unsaturated (unclipped) specular pixels and the saturated (clipped) specular pixels are marked in white and gray respectively; and (c) the plot of both clipped and unclipped pixels of two peppers in the RGB cube (the color cluster of the red pepper is marked in black and that of the yellow pepper is marked in red).

DISCUSSIONS AND FUTURE WORKS

Using the dichromatic reflection model, we have analyzed the clipping effects in color images obtained by CCD cameras. The observations drawn from this analysis brings a new understanding on images with severe color clipping effects. For example, clipped pixels define lines in the RGB color space that are parallel to the clipping axes, making quite easy to cluster these pixels together. The main implication of this clustering is in segmenting regions of interest – including regions with saturated (clipped) pixels. Another potential application of our work is in the detection and compensation of specular highlights. In a particular application of our work, we showed that good results can be achieved in segmentation when the objects are dielectric, that is, when they satisfy the dichromatic reflection model. However, that is not always the case, as for example when the target object presents a metallic texture. In our future work, we will address this shortcoming by analyzing the properties of incident and reflected light on metallic surfaces as they are sampled by CCD cameras.

	(i)	(ii)	(iii)	(iv)	(v)
(1)		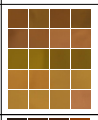	$L_R = 255$ $L_G = 182.6$ $L_B = 70.9$	$C_R = 255$ $C_G = 255$ $C_B = 99.0$	Canon Powershot G2
(2)			$L_R = 255$ $L_G = 121.1$ $L_B = 27.1$	$C_R = 255$ $C_G = 255$ $C_B = 57.1$	Canon Progressive Scan M−70
(3)		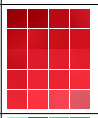	$L_R = 255$ $L_G = 21.0$ $L_B = 42.1$	$C_R = 255$ $C_G = 255$ $C_B = 127.2$	Jai CV−950
(4)		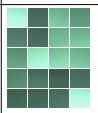	$L_R = 161.1$ $L_G = 255$ $L_B = 214.7$	$C_R = 191.3$ $C_G = 255$ $C_B = 255$	Jai CV−950
(5)	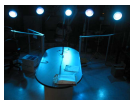		$L_R = 70.1$ $L_G = 157.3$ $L_B = 255$	$C_R = 113.6$ $C_G = 255$ $C_B = 255$	Jai CV−950
(6)			$L_R = 255$ $L_G = 132$ $L_B = 73.1$	$C_R = 255$ $C_G = 255$ $C_B = 141.2$	Sony Mavica

Table 1. Estimation of the color of illuminants (6 scenes)

Each row of the table represents a different site and/or a different illumination condition. Site (row) (1) was a parking structure with low-pressure sodium lights; site (2) had fourteen $100Watts$ high-pressure sodium lights on a bridge; sites (3), (4), and (5) were at the Purdue Robot Vision Laboratory and used respectively, red (peak at $625nm$), green ($535nm$), and blue ($425nm$) incandescent lights ($100Watts$ Sylvania Flood Par38); the hallway in site (6) has five orange ($600nm$) $100Watts$ tungsten lights. The columns on the table depict: (1) the site; (ii) 20 images of the white reference patches; (iii) the coordinates of the point L in Figure 2 (c); (iv) the coordinates of the point C in Figure 2 (c); and (v) camera sensors used in each experiment.

REFERENCES

[1] S. A. Shafer, "Using Color to Separate Reflection Components, " Color Res. Appl., 10, p. 210-218, 1985.

[2] G. J. Klinker and S. A. Shafer, T. Kanade, "The Measurement of Highlights in Color Images", Int'l J. of Computer Vision, 2(1), pp.7-32, 1988.

[3] H. Lee, "Method for Computing the Scene-illuminant from Specular Highlights," J. of Optics Society of America, A., 3(10), pp. 1694-1699, 1986.

[4] S. Tominaga, S. Ebisui, B. A. Wandell, "Scene Illuminant Classification: Brighter is better," J. of Optical Society of America, A, 18(1), pp. 55-64, 2001.

[5] S. Tominaga, "Surface Identification using the Dichrometic Reflection Model," PAMI, 13(7), 658-670, 1991.

[6] G. D. Finlayson, B. Schiele, J. L. Crowley, "Comprehensive Color Image normalization," 5th European Conf. on Computer Vision, pp.475-490, 1998.